

The shaping effect of collimated fast outflows in the Egg nebula

Dinh-V-Trung¹ Jeremy Lim

Institute of Astronomy and Astrophysics, Academia Sinica, Taiwan

trung@asiaa.sinica.edu.tw, jlim@asiaa.sinica.edu.tw

Received _____; accepted _____

submitted to ApJ

ABSTRACT

We present high angular resolution observations of the HC_3N J=5–4 line from the Egg nebula, which is the archetype of protoplanetary nebulae. We find that the HC_3N emission in the approaching and receding portion of the envelope traces a clumpy hollow shell, similar to that seen in normal carbon rich envelopes. Near the systemic velocity, the hollow shell is fragmented into several large blobs or arcs with missing portions correspond spatially to locations of previously reported high-velocity outflows in the Egg nebula. This provides direct evidence for the disruption of the slowly-expanding envelope ejected during the AGB phase by the collimated fast outflows initiated during the transition to the protoplanetary nebula phase. We also find that the intersection of fast molecular outflows previously suggested as the location of the central post-AGB star is significantly offset from the center of the hollow shell. From modelling the HC_3N distribution we could reproduce qualitatively the spatial kinematics of the HC_3N J=5–4 emission using a HC_3N shell with two pairs of cavities cleared by the collimated high velocity outflows along the polar direction and in the equatorial plane. We infer a relatively high abundance of $\text{HC}_3\text{N}/\text{H}_2 \sim 3 \times 10^{-6}$ for an estimated mass-loss rate of $3 \times 10^{-5} \text{ M}_\odot \text{ yr}^{-1}$ in the HC_3N shell. The high abundance of HC_3N and the presence of some weaker J=5–4 emission in the vicinity of the central post-AGB star suggest an unusually efficient formation of this molecule in the Egg nebula.

Subject headings: circumstellar matter: — ISM: molecules — planetary nebulae: general — stars: AGB and post-AGB—stars: individual (CRL 2688)—stars: mass loss

1. INTRODUCTION

The rapid evolution of low and intermediate mass stars (1 to 10 M_{\odot}) after the end of the Asymptotic Giant Branch (AGB) phase is accompanied by a radical change in the morphology of their circumstellar envelopes around them. The circumstellar envelope created by the slow and dusty stellar wind during the AGB phase is known to be roughly spherically symmetric as the radiation pressure on dust grains is expected to be isotropic. On the other hand, a variety of morphologies ranging from spherical to multipolar shapes have been observed in post-AGB envelopes and planetary nebulae. It is also during this phase that collimated high velocity outflows are seen, such as in the Egg nebula (Cox et al. 2000) and in CRL 618 (Sánchez-Contreras et al. 2004). The shaping of the complex envelope morphology and the mechanism that generates the high-velocity outflows of post-AGB stars are very poorly understood. Lee & Sahai (2003) suggest that envelopes with bipolar morphologies are shaped by the interactions with a fast collimated outflow or jet launched in the polar directions. Their hydrodynamic simulations are able to reproduce both the envelope morphology and other properties such as intensity of emission lines excited in the shocked gas at the interface between the jet and the slow wind.

The Egg nebula (CRL 2688) is widely considered as the prototype of proto-planetary nebulae (PPN), a class of stars in the rapid transition phase between the AGB and planetary nebulae. During the PPN phase the central post-AGB star contracts and gradually becomes hotter, but is not yet hot enough to ionize its surrounding envelope. Using high resolution spectroscopic observations of the scattered stellar light Klokova et al. (1996) determine a spectral type F5Ia for the central star with an effective temperature of $T_{\text{eff}}=6500\text{K}$. The abundance analysis reveals the enrichment of C and N together with strong enhancement of

¹on leave from Center for Quantum Electronics, Institute of Physics, Vietnamese Academy of Science and Technology, 10 DaoTan, ThuLe, BaDinh, Hanoi, Vietnam

slow neutron capture (s-process) elements, as expected for the carbon rich post-AGB star at the center of the Egg nebula.

Recently, using multi-epoch optical images from Hubble Space Telescope, Ueta et al. (2006) successfully measured the spatial expansion of the nebula and thereby determined the distance to CRL 2688 of 420 pc. We shall henceforth use this distance for the Egg nebula

High spatial resolution optical images of CRL 2688 reveal a pair of bipolar lobes seen as search-light beams emanating from the central (obscured) star and oriented perpendicular to a dark lane (Sahai et al. 1998a). This conspicuous dark lane has been commonly interpreted as an equatorial disk of cold dust. High angular resolution images of hot molecular hydrogen gas emission at $2.2\ \mu\text{m}$ reveal shocked gas, tracing the strong interaction between the fast outflows and the slow wind (Sahai et al. 1998b). Surprisingly, hot molecular hydrogen emission is seen in both bipolar lobes as well as in the equatorial plane far beyond the dark lane, indicating the presence of multiple fast collimated outflows.

Indeed, high spatial resolution mapping of CO J=2–1 emission by Cox et al. (2000) reveals the presence of several pairs of collimated fast molecular outflows along both the bipolar axis and the equatorial plane. These molecular outflows can be traced back to a common origin, presumably the location of the central post-AGB star in the Egg nebula. Cox et al. (2000) suggest that the observed CO emission does not constitute the actual fast collimated outflows, but rather molecular gas swept up by even faster collimated outflows that comprise mainly atomic or ionized gas. By contrast to its appearance in the optical, no equatorial disk is the Egg nebula is seen in the CO J=2–1 by Cox et al. (2000). High spatial resolution observation of HCN J=1–0 by Bieging & Nguyen-Q-Rieu (1996) traces molecular gas at higher densities along both the bipolar lobes and the equatorial plane consistent with gas swept up gas by the fast outflows. The only observation that seems to directly trace the AGB wind is that by Yamamura et al. (1996) in ^{13}CO J=1–0, which

does not exhibit any high velocity wings. The limited spatial resolution (about $5''$) of the observation, however, does not provide any detailed information on the structure of the circumstellar envelope.

Emission lines from cyanopolyynes molecules such as HC_3N are very prominent in the centimeter and millimeter wavelengths region toward the Egg nebula. Cyanopolyynes molecules, as large as HC_9N , have been detected (Truong-Bach et al. 1993). The line profiles of cyanopolyynes molecules do not exhibit high velocity wings, suggesting that their emission originate from the slowly expanding shell ejected during the AGB phase. Current chemical models (Millar et al. 2000, Cherchneff et al. 1993) for carbon rich envelopes suggest that HC_3N molecules are formed by photochemistry in the outer part of the expanding envelope. Thus the spatial distribution of HC_3N is predicted to exhibit a hollow shell structure. In the case of the carbon rich envelope of IRC+10216, the spatial distribution of cyanopolyynes molecules has been imaged at high angular resolution (Bieging & Tafalla 1993, Lucas & Guélin 1999, Dinh-V-Trung & Lim 2008) and shown to have the hollow shell structure as expected from chemical models. The relatively high abundance and high electric dipole moment of HC_3N make its rotational lines relatively strong in the circumstellar envelope. The HC_3N lines might be useful to probe not just the chemistry but also the structure of the envelope at high angular resolution. In the Egg nebula we also expect the molecule to form in the outer part of the envelope and its emission lines could be used to trace the spatial structure and kinematics of the outer envelope of the Egg nebula. Interferometric observation of HC_3N emission line in the 3 mm band by Nguyen-Q-Rieu & Bieging (1990) indicates a compact and centrally peaked emission, most likely due to the limited angular resolution of about $8''$.

In this paper we present high resolution observations of the HC_3N $J=5-4$ emission line, which traces the outer molecular envelope of the Egg nebula. The envelope is found to be

disrupted by the passage of the fast collimated outflows along the polar direction and in the equatorial plane. We also present a simple model of the envelope to better understand its spatial kinematics.

2. OBSERVATION

We observed the Egg nebula on 2002 November 24 and 2003 March 03 using the Very Large Array (VLA²) in its C and D configuration. We pointed the telescope at $\alpha_{J2000}=21^{\text{h}}02^{\text{m}}18.8^{\text{s}}$, $\delta_{J2000}=36^{\circ}41'38.0''$, which is very close to the peak of the continuum emission observed previously by Cox et al. (2001) and Jura et al. (2001). The rest frequency of the HC_3N J=5–4 line as compiled in the Lovas/NIST database (Lovas 2004) is 45.490316 GHz. To observe this line we configured the VLA correlator in the 2AC mode with 64 channels spanning a bandwidth of 6.25 MHz, thus providing a velocity resolution of 0.65 km s^{-1} per channel over a useful velocity range of $\sim 40 \text{ km s}^{-1}$. The total on-source integration time is about 1 hour in D configuration and about 4 hours in C configuration. We monitored the nearby quasar 21095+35330 every 5 minutes to correct for the antennas gain variations caused primarily by atmospheric fluctuations. The stronger quasar 2253+161 was used to correct for the shape of the bandpass and its variation with time. The absolute flux scale of our observations was determined from observations of standard quasars 0137+331 and 0410+769.

We edited and calibrated the raw visibilities using the AIPS data reduction package. The calibrated visibilities from different configurations were merged using the task DBCON, and then Fourier transformed to form the DIRT images. We employed the robust

²The National Radio Astronomy Observatory is a facility of the National Science Foundation operated under a cooperative agreement by Associated Universities, Inc.

weighting together with tapering of the visibilities to obtain a satisfactory compromise between angular resolution and sensitivity to extended emission. The DIRTY images were deconvolved using the clean algorithm IMAGR implemented in AIPS, providing a synthesized beam of $1''.3 \times 1''.08$ at a position angle of $PA = 2^\circ.35$. The rms noise level in our channel maps of HC_3N J=5–4 is $2.3 \text{ mJy beam}^{-1}$ in each velocity channel of 3.9 kms^{-1} . The conversion factor between the brightness temperature of the HC_3N J=5–4 emission and its flux density is $\sim 2.37 \text{ mJy K}^{-1}$. Table. 1 provides a summary of our observations.

3. RESULTS

Figure 1 shows our channel maps of the HC_3N J=5–4 emission. In Figure 2 we show the HC_3N J=5–4 line profile derived by integrating the channel maps over a region where the emission is detected above 2σ level. The HC_3N J=5–4 line has been previously observed by Fukasaku et al. (1994) with the Nobeyama 45m telescope, which has a primary beam at FWHM of about $40''$. Using the main beam efficiency provided in their paper, we estimate a conversion factor between main beam temperature and flux density of 4 Jy/K , thus giving a peak flux density of about 2 Jy for the HC_3N J=5–4 line in their observation. We measured in our observations (see Figure 2) a peak flux density for this line of $\sim 1.6 \text{ Jy}$. The shape of the line profiles in both observations are also very similar, exhibiting a near parabolic shape with a trough around the systemic velocity of -35 kms^{-1} . We conclude that our VLA observation has recovered about 80% of the emission in the HC_3N J=5–4 line present in the abovementioned single-dish observation.

In the channel maps the HC_3N J=5–4 line shows the typical characteristics of an expanding shell, i.e. the emission appears largest near the systemic velocity, and contracts toward the center at progressively higher blueshifted and redshifted velocities. The emission spans velocities between -53.9 and -19.1 kms^{-1} , from which we estimate an expansion

velocity of $\sim 17 \text{ km s}^{-1}$, that is similar to that obtained by Truong-Bach et al. (1993). At redshifted velocities between -26.9 to -19.1 km s^{-1} and the blueshifted velocities between -53.9 to -46.2 km s^{-1} the HC_3N J=5–4 emission traces a clumpy and hollow shell-like structure with radius of $\sim 4'' - 5''$. Such a hollow shell structure is expected from the prediction of HC_3N formation in the envelopes of carbon rich stars (Cherchneff et al. 1993, Millar et al. 2000). We note that similar structures have been seen most prominently in the prototypical carbon rich star IRC+10216 (Bieging & Tafalla 1993, Dinh-V-Trung & Lim 2008). The large angular size of the hollow shell and more importantly the lack of high velocity emission wings of the HC_3N J=5–4 line suggest that this line is tracing the remnant envelope created by the slow dusty wind from the central star of the Egg nebula during the AGB phase. Using the distance to the Egg nebula of 420 pc as estimated by Ueta et al. (2007), the linear size of the shell is about $3 \times 10^{16} \text{ cm}$. We note that the radius of the HC_3N shell in the archetype carbon rich envelope of IRC+10216, which is located at an estimated distance of 120 pc, is between $15''$ to $20''$. If IRC+10216 was located at the same distance as the Egg nebula, the HC_3N shell would have a radius of $4''$ to $6''$. Assuming that the interstellar radiation field is the same for both objects, the similarity in size of the HC_3N shell in both the Egg nebula and IRC+10216 suggests that the mass loss rate in both objects is comparable. The mass loss rate of IRC+10216 is estimated to be in the range 1 to $3 \times 10^{-5} \text{ M}_{\odot}/\text{yr}$ from the modeling results of Crosas & Menten (1997), Dinh-V-Trung & Nguyen-Q-Rieu (2000) and Schoier et al. (2002). The comparably high mass loss rate of the central star in the Egg nebula at the time it produced the observed envelope suggests that this period might correspond to the superwind phase the end stage of the evolution on AGB.

Near the systemic velocity, most prominently at and between velocity channels -30.7 and -38.4 km s^{-1} , the hollow shell structure is clearly disrupted and fragmented into several large clumps of intense HC_3N J=5–4 emission. At the systemic velocity the shell is

delineated by four large clumps roughly mirror-symmetric with respect to the lines passing through the nebula center at position angles of $\sim 20^\circ$ and 110° . The space between these clumps form two pairs of cavities. Figure 3 shows the integrated intensity map of the HC_3N J=5–4 emission. This integrated intensity map clearly shows the presence of the cavity pair in the equatorial plane and also the pair along the polar direction. These cavities are separated by four intense peaks of HC_3N emission. These evacuated cavities are oriented along the axes of the fast collimated outflows as traced by the molecular hydrogen emission (Sahai et al. 1998b) and CO J=2–1 emission (Cox et al. 2000) as sketched in Figure 3. As can be seen in the figure, the spatial correspondance between the cavities and the fast outflows is reasonably good. These fast outflows are confined within the cavities. That is especially evident for the outflows in the polar direction, which are closely aligned within the narrow cavities oriented at a position angle of about 20° . We note that Cox et al. (2000) estimate the average position angle of the polar outflows to be about 17° , very similar to that of the cavities seen in our HC_3N J=5–4 observations. Cox et al. (2000) also suggest that all the outflows can be traced back to a common origin. As can be seen in Figure 3, the intersection of different outflows is clearly offset from the center of the HC_3N shell. Close inspection of Figure 3 indicates that the shell is centered close to the position of the 1.3 mm continuum peak ($\alpha_{j2000}=21\text{h}02\text{m}18.647\text{s}$, $\delta_{j2000}=36\text{d}41\text{m}37.8\text{s}$) observed by Cox et al. (2000). We estimate that the offset between the intersection of outflows and the center of the HC_3N shell is about $\sim 1''$, which is quite significant given our high angular resolution of $\sim 1''.3$. If the outflows indeed have a common source, that source might have moved in the envelope. The dynamical age of the outflows estimated by Cox et al. (2000) ranges from 125 years to 1000 years. Even if the source moves at a relatively slow speed of 2 kms^{-1} , its position could change by as much as $1''$ in 1000 years.

Interestingly, HC_3N J=5–4 emission is also found close to center of the Egg nebula in several velocity channels between -30.7 to -42.3 kms^{-1} , forming a faint bridge between

the Northern and Southern portions of the shell. The existence of HC_3N in the inner envelope is difficult to understand within the framework of current chemical models. Previous observations by Audinos et al. (1994) show that HC_3N emissions from higher lying transitions in the 2 mm and 1 mm band, which are excited mainly under warmer and denser conditions, peak at the center of the carbon rich envelope IRC+10216, implying the much enhanced abundance of HC_3N toward the center of the envelope. For the lower lying transition $J=5-4$ to be seen toward the center of the envelope, the abundance of HC_3N needs to be even higher because of the lower optical depth in comparison to higher J transitions. This suggests that the formation of HC_3N is quite efficient in the inner dense region of the envelope where photodissociation of molecular species is low. There are two main differences in comparison to the archetypical envelope of IRC+10216: the center of the Egg is likely quite disturbed because of the passage of fast outflows and the central hotter (F-type) post-AGB star emits more UV photons. These differences might contribute to the enhanced efficiency of HC_3N formation.

4. A simple model of HC_3N shell

From the discussion in the preceding section we suggest that HC_3N emission traces the remnant AGB envelope around the Egg nebula. The AGB envelope is disrupted by the interaction with the fast collimated outflows. These outflows open channels or cavities along the polar and equatorial directions. Thus the HC_3N $J=5-4$ emission is very useful in providing complementary information to previous observations on the structure of the Egg nebula. To gain more insight on the structure of the nebula and to estimate the abundance of HC_3N , we construct a simple model of the HC_3N shell. In Figure 4. we show a sketch of the overall structure of the HC_3N shell. The hollow shell is filled with the remnant AGB wind, which is assumed to be spherically symmetric. Collimated fast outflows emanate

from the central post-AGB star along both polar and equatorial directions. These outflows interact with the slow AGB wind, entraining molecular gas along their path. As a result, the remnant AGB envelope is disrupted and two pairs of cavities are excavated by the fast collimated outflow. For simplicity, we assume that the abundance of HC_3N is constant over the whole hollow shell. We do not take into account the presence of HC_3N J=5–4 emission near the center of the nebula because a correct derivation of the abundance and spatial distribution would require more constraints from multiline observations. We also assume that the HC_3N J=5–4 line forms under the LTE condition with a temperature of 30 K. Although the LTE assumption might be quite crude in the circumstellar envelope environment, it is commonly used to estimate the relative abundance of molecules. For our purpose of studying the spatial kinematics and estimate of the abundance, that assumption should be adequate. When multi-line observations are available, more elaborate model can be constructed. We project a spherical hollow shell into a 3-dimension regular grid. We adopt an expansion velocity of 15 km s^{-1} for the shell. The gas density at each radial point in the shell is calculated from the mass loss rate. We adopt the mass loss rate of $3 \times 10^{-5} \text{ M}_{\odot} \text{ yr}^{-1}$ estimated in the previous section. The turbulence velocity, which defines the local linewidth, is assumed to be 1 km s^{-1} as is commonly used for circumstellar envelopes. The intensity of the HC_3N J=5–4 line is calculated by solving directly the radiative transfer equation along each line of sight. We then use the emerging intensity to form the model channel maps. The channel maps are then convolved with the synthesized beam of our VLA observation. The resulting model channel maps can be then compared directly with our observation. We use a inclination angle of 15° for the envelope, which is almost the same as derived from the model of Yusef-Zadeh et al. (1984). The opening angle of the cavities in the both the polar direction and in the equatorial plane is 40° . The position angle of the nebular axis on the plane of the sky is set to 20° , which is close to that advocated by Cox et al. (2000). The complex distribution of HC_3N does not allow a more accurate estimate

of the position angle. Besides, there are several outflows contributing to the cavities in the polar direction, making the definition of the position angle somewhat ill-defined. The parameters of our simple model are collected in Table. 2.

In Figure 5 we show the channel maps of the HC_3N J=5–4 emission calculated with our model. The main features found in the observed channel maps, namely the cavities and the changing morphology of the emission between velocity channels, are qualitatively reproduced in our model. The predicted total intensity profile of the HC_3N J=5–4 line is shown in Figure 6. The predicted line profile is similar to that seen in the single dish observation of Fukasaku et al. (1994) and also in our observations. The observed strength (about 2 Jy at the peak intensity) and the parabolic shape with a depression around the systemic velocity, which is caused by the presence of the two pair of cavities, of this line is also reproduced with our model. .

5. Summary

We have imaged at high angular resolution the distribution of HC_3N J=5–4 emission line in the Egg nebula. We find that in the approaching and receding portion of the envelope the HC_3N emission traces a clumpy hollow shell structure, similar to that seen in normal carbon rich envelopes. Near the systemic velocity, however, the hollow shell is fragmented into several large blobs or arcs. The missing portions of the hollow shell correspond spatially to locations of the high velocity outflows observed previously in the Egg nebula. We also find that the intersection of fast molecular outflows previously suggested as the location of the central post-AGB star is significantly offset from the center of the hollow shell. We interpret the observed spatial-kinematics of HC_3N J=5–4 emission as the direct evidence for the disruption of the slowly expanding envelope ejected during the AGB phase by the interaction with collimated high velocity outflows initiated during the transition. From

modelling the HC_3N distribution we could reproduce qualitatively the spatial kinematics of the HC_3N J=5–4 emission using a HC_3N shell with two pairs of cavities with opening angle of $\sim 40^\circ$ opened by the collimated high velocity outflows along the polar direction and in the equatorial plane. We infer a relatively high abundance of $\text{HC}_3\text{N}/\text{H}_2 \sim 3 \times 10^{-6}$ for an estimated mass loss rate of $3 \times 10^{-5} \text{ M}_\odot \text{ yr}^{-1}$. The high abundance of HC_3N and the presence of some weaker J=5–4 emission in the vicinity of the central post-AGB star suggest an unusually efficient formation of this molecule in the Egg nebula.

We thank the VLA staff for their help with the observations. This research has made use of NASA’s Astrophysics Data System Bibliographic Services and the SIMBAD database, operated at CDS, Strasbourg, France.

REFERENCES

- Audinos, P., Kahane, C., Lucas, R., 1994, A&A 287, L5
- Bieging, J.H., Tafalla, M., 1993, AJ 105, 576
- Bieging, J.H., Nguyen-Q-Rieu, 1996, AJ, 112, 706
- Cherchneff, I., Glassgold, A., Mamon, G., 1993, ApJ 410, 188
- Chiu, P.J., Hoang, C.T., Dinh-V-Trung, et al., 2006, ApJ 645, 605
- Cox, P., Lucas, R., Huggins, P.J., Forveille, T., Bachiller, R., Guilloteau, S., Maillard, J.P., Omont, A., 2000, A&A 353, L25
- Crampton, D., Cowley, A.P., Humphreys, R.M., 1975, ApJ, 198, L135
- Crosas, M., Menten, K., 1997, ApJ 483, 913
- Dinh-V-Trung, Nguyen-Q-Rieu, 2000, A&A 361, 601
- Dinh-V-Trung, Lim, J., 2008, ApJ 678, 303
- Fakasaku, S., Hirahara, Y., Masuda, A., et al., 1994, ApJ 437, 410
- Jura, M., Turner, J.L., van Dyk, S., Knapp, G.R., 2001, ApJ 528, L105
- Klochova, V.G., Szczerba, R., Panchuck, V.E., 2000, Astr. Lett., 26, 439
- Knapp, G.R., Sandell, G., Robson, E.I., 1993, ApJS, 88, 173
- Latter, W.B., Hora, J.L., Kelly, D.M., Duetsch, L.K., Maloney, P.R., 1993, AJ, 106, 260
- Lee, C.F., Sahai, R., 2003, ApJ 586, 319
- Lovas, F.J., 2004, J.Phys.Chem.Ref.Data, 33, 177

- Lucas, R., Guélin, M., 1999, IAU Symposium 191, edited by T. Le Bertre, A. Lebre and C. Waelkens, p. 305
- Millar, T.J., Herbst, E., Bettens, R.P.A., 2000, MNRAS 316, 195
- Ney, E.P., Merrill, K.M., Becklin, E.E., Neugebauer, G., Wynn-Williams, C.G., 1975, ApJ 198, L129
- Nguyen-Q-Rieu, Bieging, J., 1990, ApJ 359, 131
- Sahai, R., Trauger, J.T., Watson, A.M., et al. 1998, ApJ 493, 301
- Sahai, R., Hines, D., Kastner, J.H., et al., 1998, ApJ 492, L163
- Schoier, F., Ryde, N., Olofsson, H., 2002, A&A 391, 577
- Truong-Bach, Graham, D., Nguyen-Q-Rieu, 1993, A&A 277, 133
- Ueta, T., Murakawa, K., Meixner, M., 2006, ApJ, 641, 1113
- Yamamura, I., Onaka, T., Kamijo, F., Deguchi, S., Ukita, N., 1996, ApJ, 465, 926
- Yusef-Zedeh, F., Morris, M., White, R.L., 1984, ApJ 278, 186

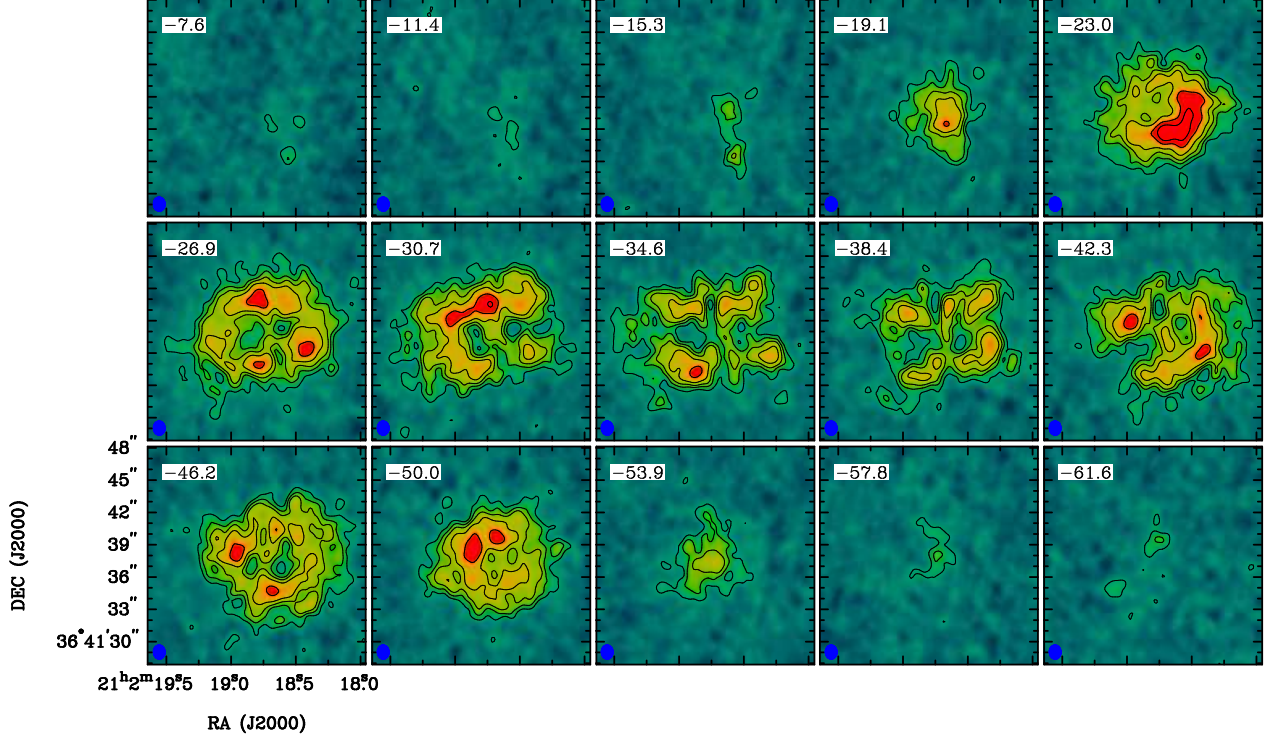


Fig. 1.— Channel maps of the HC_3N $J=5-4$ emission from the Egg nebula in contour and grayscale. The contour levels are $(3, 5, 7, 10, 15, 20)\sigma$ where the rms noise level $\sigma = 2.3$ mJy beam $^{-1}$. The synthesizer beam of $1''.3 \times 1''.08$ is shown in the lower left of the upper left frame. The conversion factor between the brightness temperature and the flux density of the HC_3N $J=5-4$ emission is 2.37 mJy K $^{-1}$.

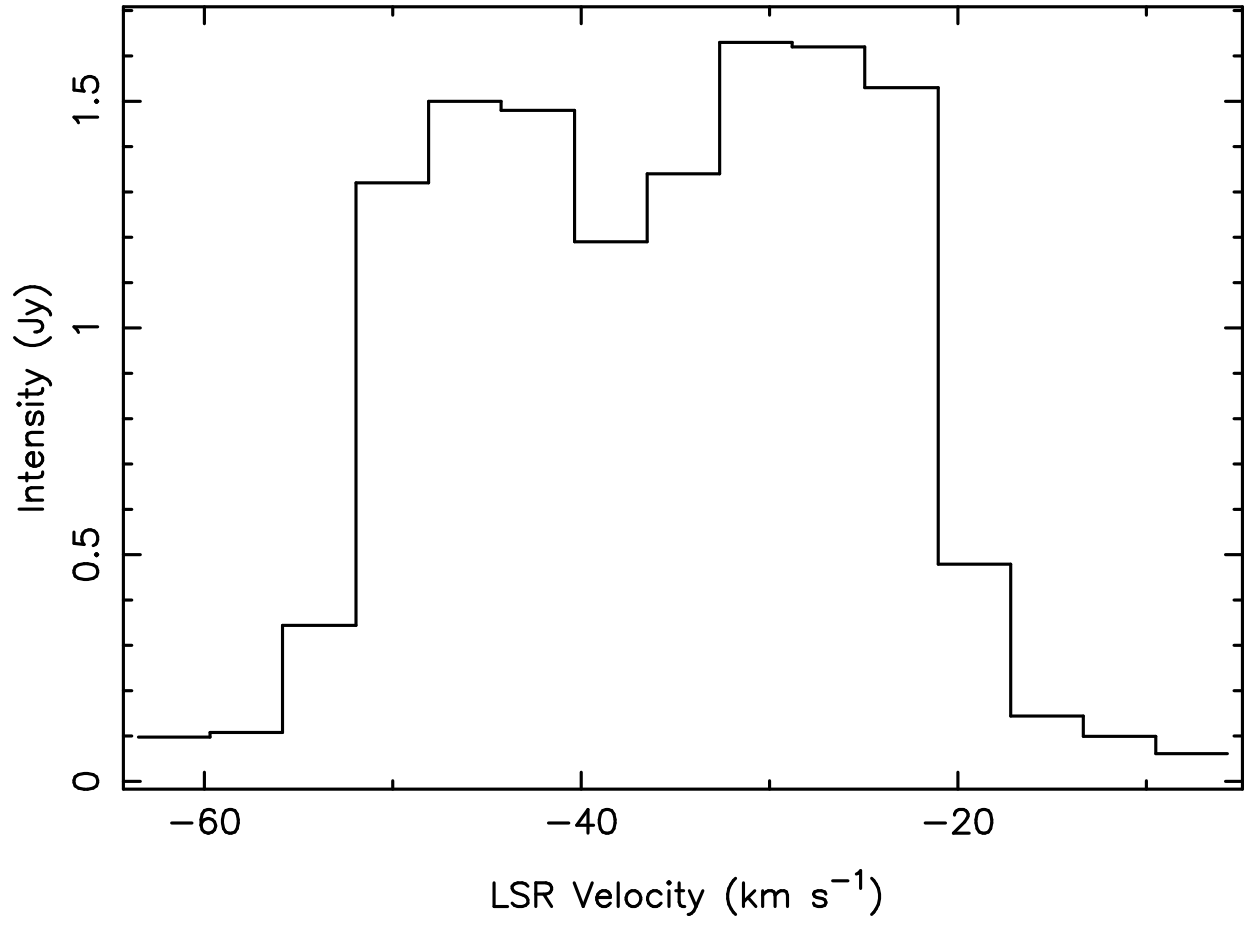


Fig. 2.— Total intensity profile of the HC_3N J=5-4 line from the Egg nebula.

Table 1: Summary of the observations

Line	HC ₃ N J=5–4
Rest frequency	45.490316 GHz
Obs. date/Config.	24 Nov 2002
	C configuration, 4 hours on-source time
	10 Mar 2003
	D configuration, 1 hour on-source time
Synthesized beam	1.3'' x 1.08'' at PA = 2°.35
ΔV	3.9 kms ⁻¹
rms noise	2.3 mJy beam ⁻¹

Table 2: Model parameters.

Distance	420 pc
Mass loss rate	3 10 ⁻⁵ M _⊙ yr ⁻¹
Expansion velocity	17 kms ⁻¹
[HC ₃ N]/[H ₂]	3 10 ⁻⁶
Inner radius of HC ₃ N shell	10 ¹⁶ cm
Outer radius of HC ₃ N shell	4 10 ¹⁶ cm
Turbulence velocity	1 kms ⁻¹
Opening angle of bipolar lobes	40°
Opening angle of equatorial cavities	40°
Inclination angle	15°
Position angle of bipolar lobes	20°

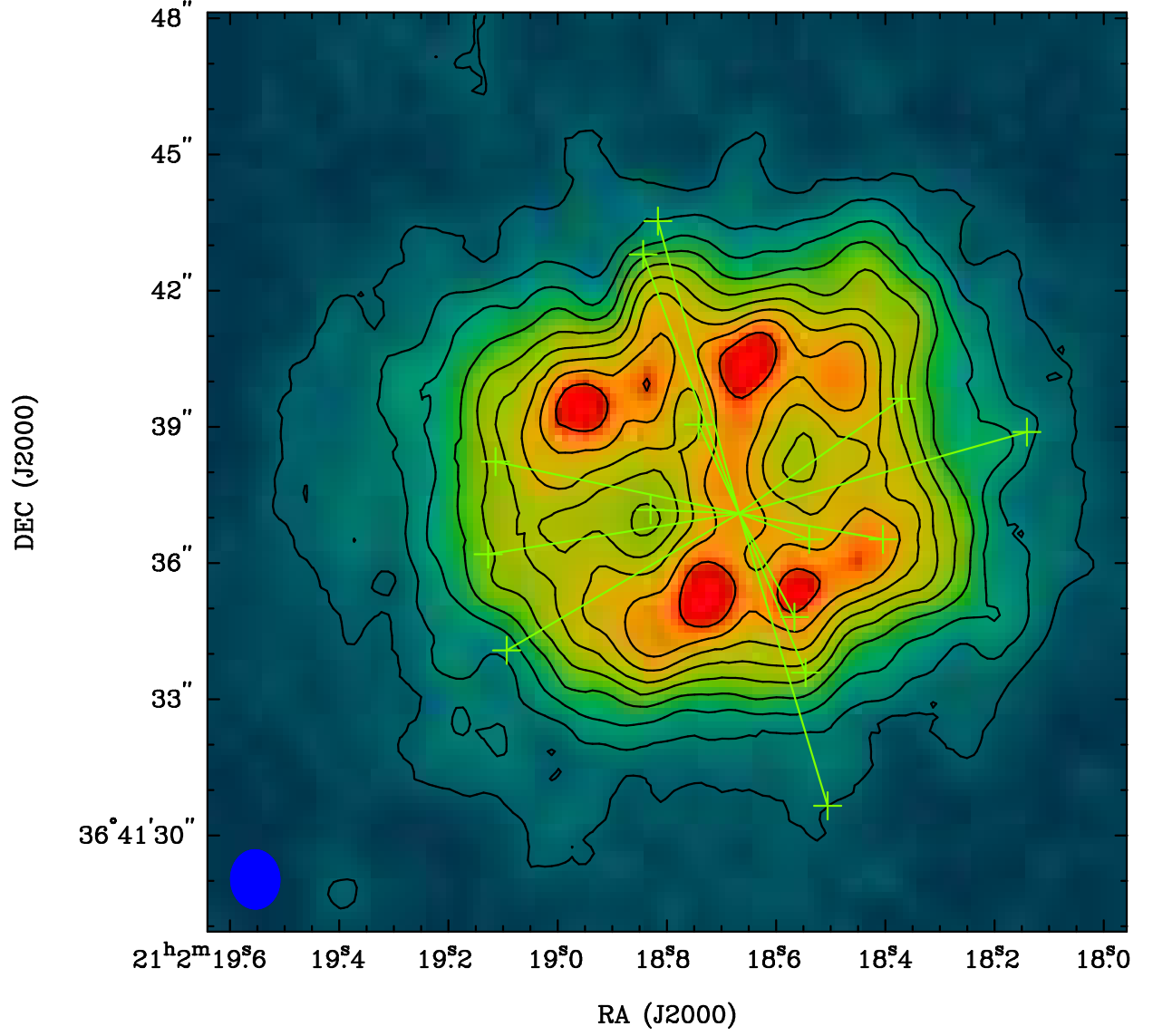


Fig. 3.— The integrated intensity map of the HC₃N J=5–4 line from the Egg nebula. The contour levels start from 0.1 Jy km s^{−1} in step of 0.1 Jy km s^{−1}. The high velocity outflows identified by Cox et al. (2000) are marked with crosses and solid lines.

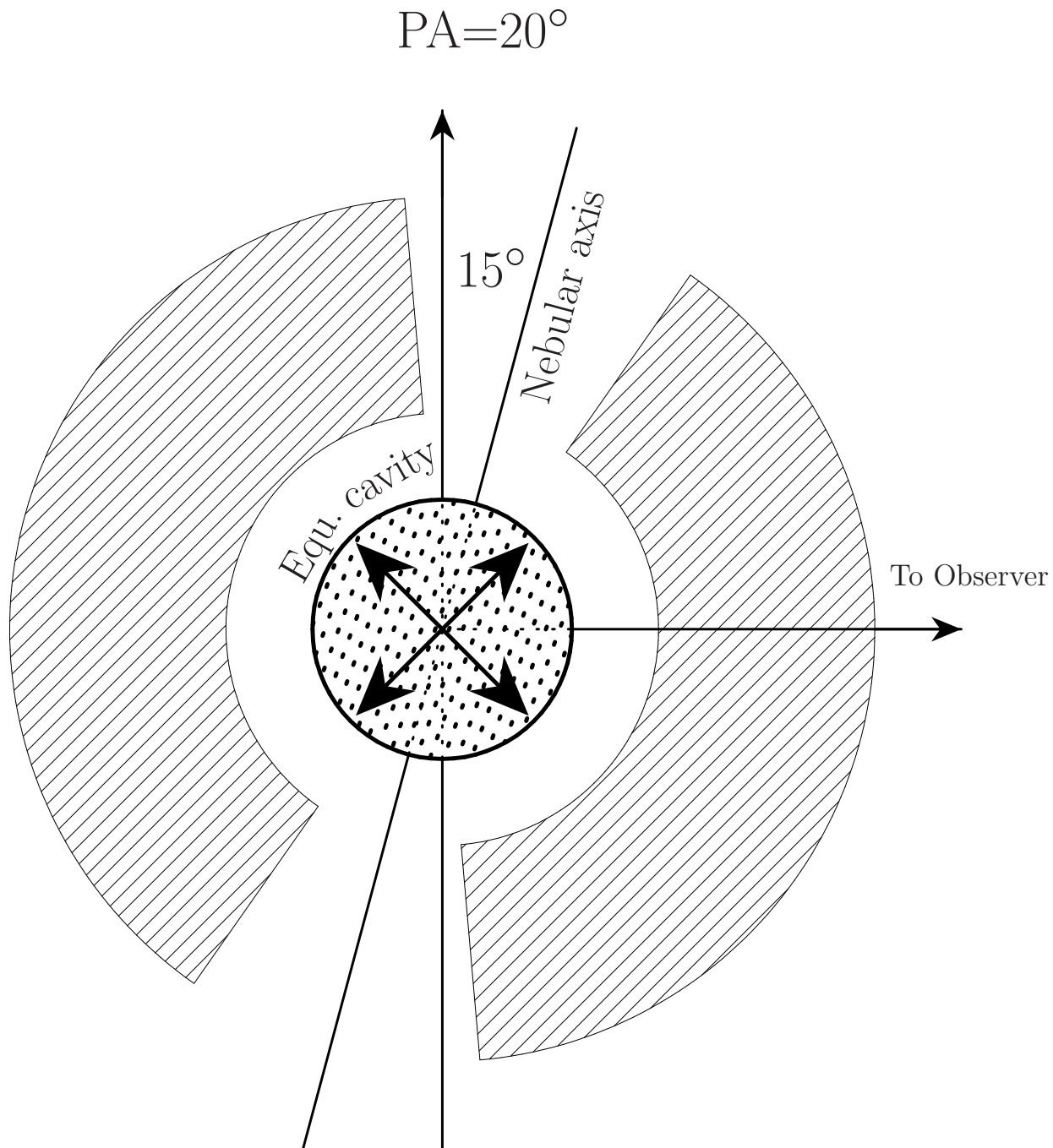


Fig. 4.— Sketch of the HC_3N shell in the Egg nebula. The spherical shell has holes or cavities along the polar directions and in the equatorial plane due to the disruptive effect of the high velocity jets.

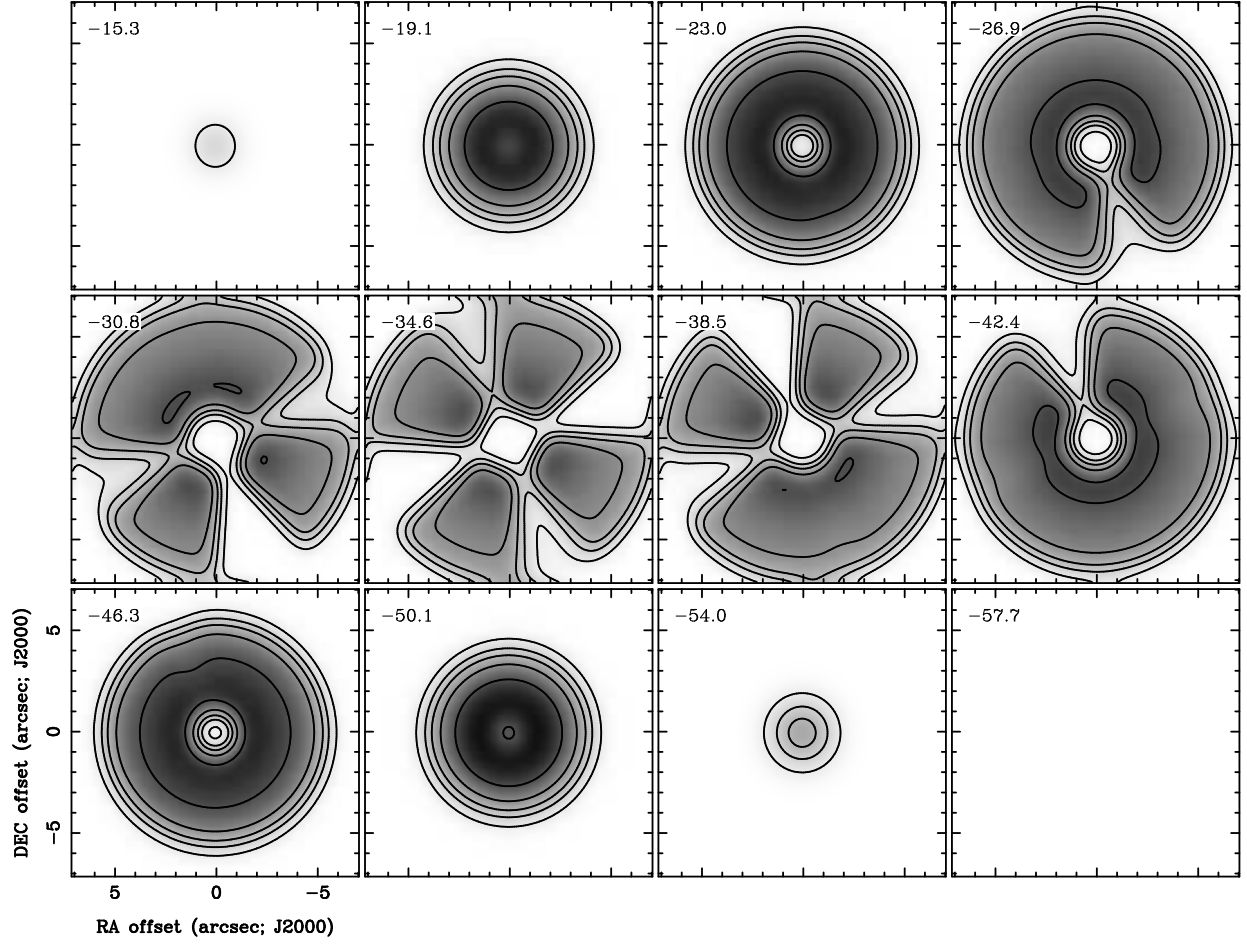


Fig. 5.— Channel maps of HC_3N $J=5-4$ emission calculated with our model and convolved with the same gaussian beam as the synthesized beam of our VLA observations. The emission is shown in both greyscale and in contours. The contour levels are the same as in Figure 1.

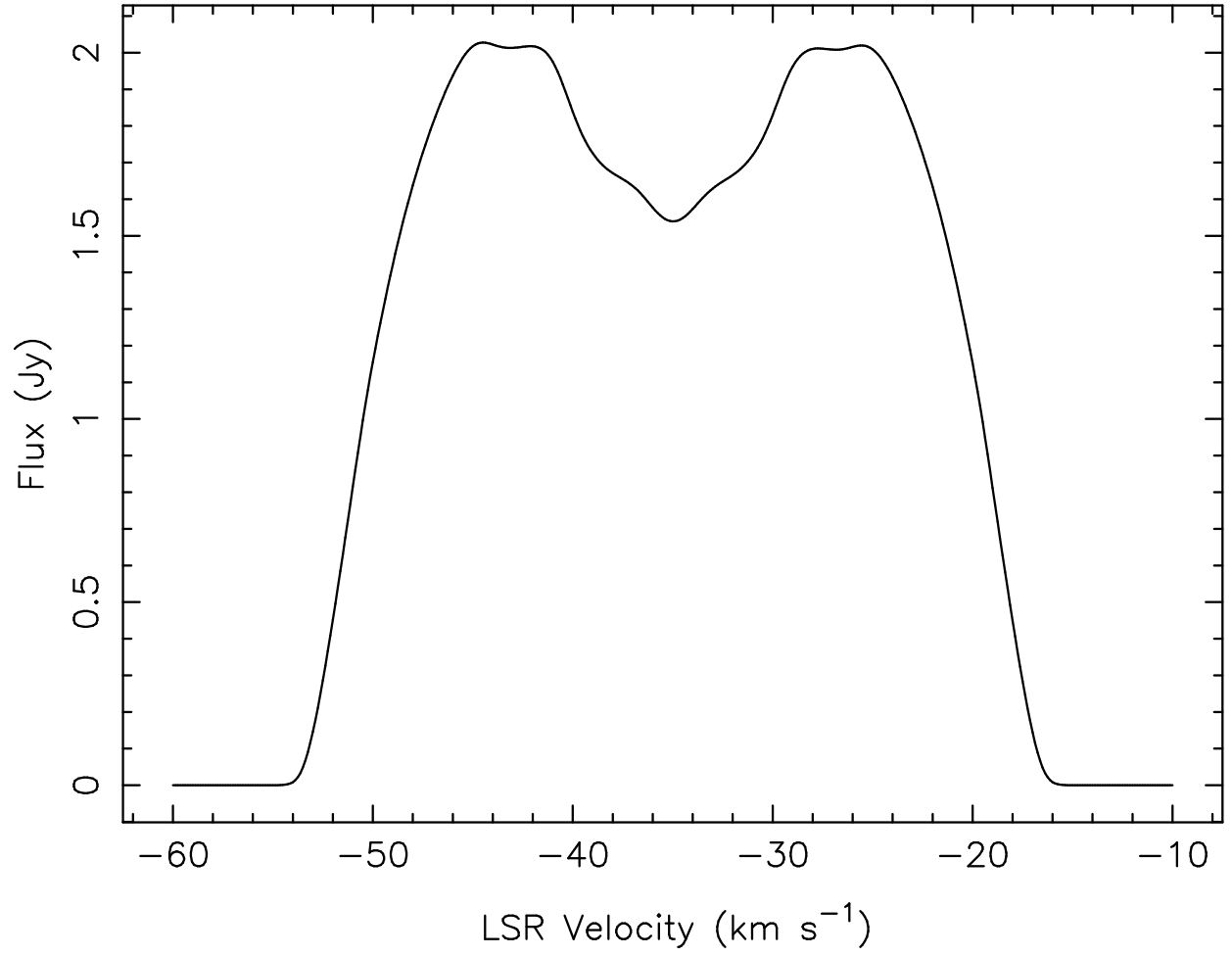


Fig. 6.— Predicted total intensity profile of the HC_3N J=5-4 line.